Carbon Nanotubes Reorganize Actin Structures in Cells and ex Vivo

ARTICLE *in* ACS NANO · AUGUST 2010

Impact Factor: 12.88 · DOI: 10.1021/nn101151x · Source: PubMed

ARTICLE

Carbon Nanotubes Reorganize Actin Structures in Cells and *ex Vivo*

Brian D. Holt,[†] Philip A. Short,[†] Andrew D. Rape,[†] Yu-li Wang,[†] Mohammad F. Islam,[‡,§,*] and Kris Noel Dahl[†,‡,*]

[†]Department of Biomedical Engineering, [‡]Department of Chemical Engineering, and [§]Department of Materials Science & Engineering, Carnegie Mellon University, 5000 Forbes Avenue, Pittsburgh, Pennsylvania 15213-3890

ABSTRACT The ability of globular actin to form filaments and higher-order network structures of the cytoskeleton is essential for cells to maintain their shape and perform essential functions such as force generation, motility, and division. Alterations of actin structures can dramatically change a cell's ability to function. We found that purified and dispersed single wall carbon nanotubes (SWCNTs) can induce actin bundling in cells and in purified model actin systems. SWCNTs do not induce acute cell death, but cell proliferation is greatly reduced in SWCNT-treated cells with an increase in actin-related division defects. Actin, normally present in basal stress fibers in control cells, is located in heterogeneous structures throughout the SWCNT-treated cell. These SWCNT-induced changes in actin structures are seen functionally in multinucleated cells and with reduced force generation. *Ex vivo*, purified actin filaments cross-linked with α-actinin and formed isotropic networks, whereas SWCNTs caused purified actin filaments to assemble into bundles. While purified, isolated SWCNTs do not appear acutely toxic, this subcellular reorganization may cause chronic changes to cellular functions.

KEYWORDS: carbon nanotube · cytoskeleton · actin · toxicity · mitosis

Nanomaterials have been at the forefront of technology for a myriad of diverse applications, but their effects on biological systems have not been thoroughly studied. Long lasting toxicity of new chemical and material technologies often presents in ways not detectable by standard toxicity tests. Single wall carbon nanotubes (SWCNTs) are the newest class of the carbon materials and are used in many technological applications due to their small size, large surface area, low density, stability, and rigidity.[1,2] Indeed, significant efforts have been recently focused on biological applications of SWCNTs as gene or drug transporter, labeling agents for intracellular components, *etc.*[3−7] However, there is disagreement as to their cellular toxicity.[8] Carbonaceous impurities (*e.g.*, amorphous carbon, graphitic materials, fullerenes, *etc.*) and metallic catalyst particles present in unpurified SWCNT samples are toxic to cells.[9,10] In addition, the bundling of SWCNTs induced by van der Waals forces has deleterious effects on cellular focal adhesions,[11,12] cell shape,[13] proliferation, and differentiation.[14] On the other hand, purified and dispersed SWCNTs have been used to deliver drugs and protein into cells without causing significant cellular toxicity.[2,15,16] In this work, we report that purified and dispersed single-wall carbon nanotubes (SWCNTs) are not acutely toxic to cells but have an impact on actin structures with numerous downstream cellular effects.

Inside cells globular actin (G-actin), an abundant ubiquitous protein, can self-assemble into filaments (F-actin) of diameter ~7 nm and lengths of tens of micrometers. F-actin can then organize into higher-ordered networks and bundles in eukaryotic cells with a host of accessory proteins to create spatially and temporally unique regions of actin structures which play vital roles in cell shape, motility, force generation, division, and many other cell functions. Similar in size to F-actin, SWCNTs have diameters of ~1 nm and lengths ranging from 100 nm to a few micrometers.

Here, we use a high concentration of highly purified, dispersed SWCNTs and visualize macromolecular changes inside of cells using laser scanning confocal microscopy. We find a dramatic redistribution of actin from basal stress fibers in control cells to heterogeneous structures distributed throughout the cell including plaques of actin at the apical surface in SWCNT-treated cells. We also observe a significant reduction in cell proliferation and force generation. *Ex vivo*, actin forms bundles of filaments in the presence of SWCNTs, confirmed by bundling assays and confocal imaging. This may explain the previous observation of reduced cell adhesion.[13]

RESULTS AND DISCUSSION

Dispersed SWCNTs Reduce Cell Proliferation. In our experiments, we used highly purified

*Address correspondence to krisdahl@cmu.edu, mohammad@cmu.edu.

Received for review May 24, 2010 and accepted July 21, 2010.

Published online July 29, 2010. 10.1021/nn101151x

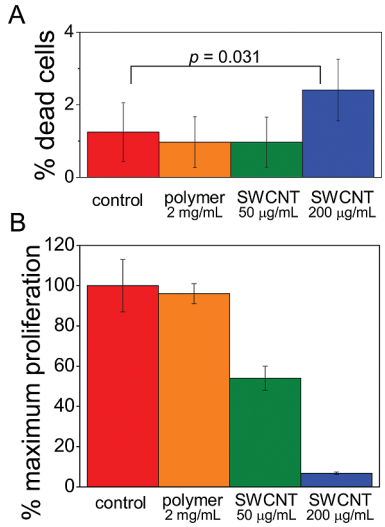

Figure 1. Isolated and purified SWCNTs were not acutely toxic to HeLa cells but reduced cell proliferation after two days of exposure. (A) Cell death was measured by propidium iodide uptake and normalized by the cell permeant DNA stain Hoechst 33342. High levels of the polymer used to disperse the SWCNTs (orange) and 50 μg/mL SWCNTs (green) were statistically similar to the control (red) with $p > 0.05$. Treatment with 200 μg/mL SWCNT (blue) resulted in a slightly higher cell death, but not indicative of SWCNTs being an acutely toxic substance. (B) HeLa cells, seeded at the same density for each group and treated with SWCNTs for 2 days, showed a dose-dependent reduction in proliferation as measured by a cell enumeration assay. Here, proliferation is presented as a percentage of the number of cells present in the control sample. Cells were imaged at 20× magnification with 1000−5000 cells per sample (1000 minimum in reduced proliferation case). Error bars are SEM.

SWCNTs dispersed in water using a biocompatible triblock copolymer Pluoronic F127. Highly purified SWCNTs were chosen to minimize any impurity-induced toxic effects.[10] In addition, we chose SWCNTs of an average length of 145 ± 17 nm with diameters ranging from 0.7−1.3 nm for increased cellular uptake, since nanotubes with lengths <190 nm have a higher probability to enter cells compared to longer SWCNTs.[17] We first tested whether our purified and dispersed SWCNTs were acutely toxic to cells. We exposed HeLa cells to SWCNT solutions for 2 days and measured changes in cell viability and subcellular structures using fluorescence techniques. To identify dead cells, we exposed control and treated HeLa cells to propidium iodide (PI) and counted the number of PI positive cells. PI, a membrane impermeable nuclear dye, identifies dead cells by labeling cells that have lost membrane integrity, such as necrotic or late apoptotic cells. Figure 1A shows that exposure to F127 polymer or to low concentrations of SWCNTs (50 μg/mL) did not show significant cell death compared to control cells. High concentrations of SWCNTs, for example, 200 μg/mL, caused a slightly higher level of cell death (p = 0.031 by Student's t test) compared with control, but this level of cell death is not indicative of SWCNTs being an acutely toxic substance. HeLa cells are adherent and often detach into the media after extensive disruption of focal adhesions or death. As such, we also investigated the media for any detached cells or signs of ruptured cell components but did not observe a significant number of cells or cell fragments in any population tested (see Materials and Methods). We did not observe any changes in nuclear morphology including DNA condensation or fragmentation, also suggesting that there was no late apoptosis (described further below). However, in measurements of populations of cells over time, we found that SWCNT-treated cells had a dramatic dose-dependent reduction in cell proliferation after 2 days (Figure 1B).

SWCNTs Reorganize Actin Structures and Focal Adhesions within Cells. While visualizing fixed cells, we observed that ~60% of all SWCNT-treated cells showed cytokinetic division defects, such as giant cells, multinucleated cells, incomplete cytokinesis, or an observable cleavage furrow (Supporting Information, Figure 1), suggesting that cells are not able to proceed through cell division. In contrast, only ~10% of untreated HeLa cells or cells treated with F127 polymer showed any division defects. We have used SWCNT:F127 at a ratio of both 1:10 and 1:20, and an excess of F127 did not affect SWCNTs affects on actin reorganization or cellular division defects. It is possible that cells were arrested in late cytokinesis because SWCNTs stabilized the actin filaments recruited to the cleavage furrow,[18] and the actin could not disassemble to allow the cell to proceed through cell division. Alteration of actin structures could also explain phenotypes of giant cells.

We imaged actin structures inside of cells using rhodamine phalloidin-labeled actin filaments by both fluorescence widefield and confocal microscopy. Widefield imaging of confluent monolayers of treated cells showed that actin filaments inside of SWCNT-treated cells were greatly redistributed compared with control cells (Figure 2A). Actin structures at the middle focal-plane of untreated cells were present only at the cortex of the cells, whereas SWCNT-treated cells showed actin throughout the interior of the cells in spiky perinuclear projections. Imaging of isolated cells also showed significant reorganization of actin and changes in cell morphology (Supporting Information, Figure 2).

Confocal imaging in the $x-z$ plane of isolated cells confirmed that the cellular actin filaments, which are normally localized to basal stress fibers, were heterogeneously redistributed to the cellular interior (Figure 2B). We then quantified localization of actin filaments in control and SWCNT-treated cells by measuring the fluorescence intensity of rhodamine phalloidin from 10 cells normalized to cell height (Figure 2C; there is no statistical difference in cell height between control and treated cells). The size of the error bars for SWCNT-treated cells are indicative of large heterogeneity of F-actin distribution compared to control. The significantly larger area under the curve for SWCNT-treated

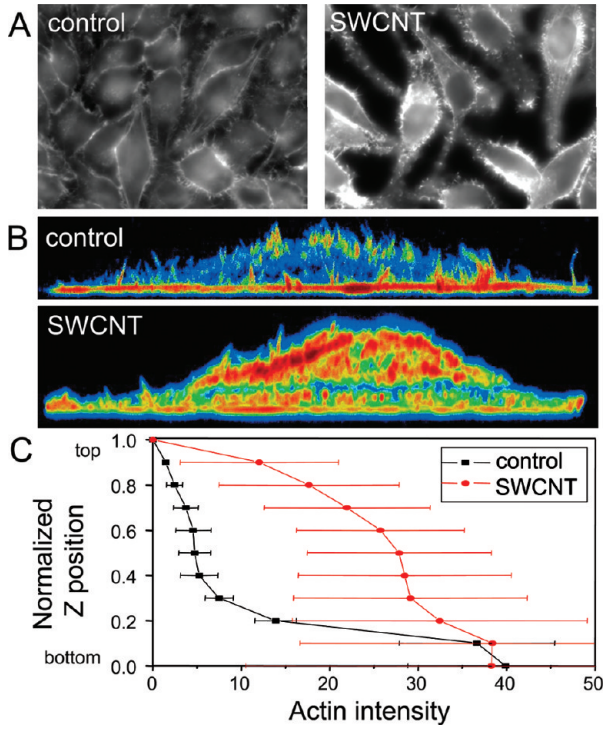

Figure 2. High resolution imaging shows reorganization of rhodamine phalloidin-labeled actin inside of SWCNT-treated cells. (A) Widefield view of the *x*−*y* plane of control cells imaged at the midline of the cell shows actin at the cortex or edge of the cell. In contrast, SWCNT-treated cells show intracellular, perinulear spiky actin projections with little order. (B) Confocal imaging of isolated cells in the *x*−*z* plane (compressed in the *y*-direction) with pseudocolor for rhodamine phalloidin intensity highlights the reorganization of actin. In control cells, actin was most concentrated in the stress fibers along the basal layer of the cell. SWCNT-treated cells had strong actin density throughout the cell, losing the preferential localization. (C) We have quantified the localization of actin densities in cells. In control cells, the actin was concentrated at the basal layer of the cell, whereas in SWCNT-treated cells actin was found throughout the cell. The change in standard deviation between the control and SWCNT-treated cells highlighted the regular distribution in control cells and the heterogeneous distribution of actin throughout SWCNT-treated cells. (n = 15 control, 10 SWCNT-treated).

cells, which is the total fluorescence intensity and hence proportional to total F-actin, is possibly due to a G- to F-actin shift or an upregulation of actin.

Actin structures may be reorganized by SWCNTs or focal adhesions may be "attracted" to the localized stiffness induced by SWCNTs at the apical surface during treatment and cause the subsequent formation of stress fibers. To determine the mechanisms by which actin may be reorganized in cells we transfected cells with GFP-paxillin and imaged changes associated with SWCNT treatment. Control HeLa cells showed typical actin−paxillin structures with actin stress fibers terminating at punctate paxillin focal adhesions (Figure 3A,B and Supporting Information, Figure 3). Cells treated for 2 days with 200 μg/mL SWCNTs showed redistribution of paxillin structures (Figure 3A,B and Supporting Information, Figure 3). We measured an effective time-course of actin (measured with GFP-moesin) and paxillin (GFP-paxillin) relocalization at early times (order of hours) in single cells to determine temporal events in SWCNTs' reorganization of cytoskeletal structures. We found that actin was initially redistributed to the apical surface as plaques (Figure 3C). Slightly later, paxillin was redistributed to the apical surface (Figure 3B). We suggest that SWCNTs affect actin as well as paxillin, but actin structures are altered prior to paxillin redistribution and to a lesser degree (Figure 3D), although basal changes in paxillin may appear earlier. Since we purposefully selected for small (~150 nm) SWCNTs, it is unlikely that small points could be acting as zones of increased stiffness.

Functional Cytoskeleton Changes with SWCNT Addition. Since actin structures and, to a lesser extent, paxillin structures were reorganized in SWCNT-treated cells, we tested for functional changes related to force generation. We have already observed functional cellular changes including three-dimensional actin organization, some giant cells, and multinucleation as well as general changes in cell proliferation. To measure force generation, we seeded NIH-3T3 cells on polyacrylamide hydrogels with micropatterned adhesive 50 μm squares (Figure 4A). A molecular layer of patterned gelatin was covalently attached to the polyacrylamide gel and allowed us to obtain samples of homogeneous shape and size. NIH-3T3 fibroblasts were chosen since they generate large traction forces on the substrate to which they adhere.[19] By imaging fluorescent latex beads in the polyacrylamide gel and tracking the movement of the beads before and after the cell is removed, we were able to produce intensity color maps representing the spatially varying stress produced inside the cell boundary (Figure 4B). Force generation is significantly reduced in SWCNT-treated cells, particularly at the corners. The maximum levels of traction stresses generated by the cell, quantified as the 95 percentile traction stress or the average magnitude of the highest 5% of stresses, is reduced in SWCNT-treated cells (Figure 4C). Also, the average traction stress is significantly reduced with increased SWCNT treatment time (Figure 4D).

SWCNTs Bundle Purified F-Actin. The cytoplasm is a complex and dynamic environment, and actin reorganization in the cell could be due to many indirect factors. To explore a more direct interaction between SWCNTs and actin filaments, we performed centrifugation and imaging assays with purified actin filaments *ex vivo*. We added variable amounts of SWCNTs to F-actin and isolated cross-linked and bundled actin using low-speed centrifugation (12000*g*). At this speed individual actin filaments and SWCNTs alone did not pellet or sediment. Increasing amounts of SWCNTs in F-actin solutions effectively promoted bundling of increasing amounts of F-actin, as illustrated in Figure 5A. Similar experiments with SWCNTs and bovine serum albumin (BSA) did not show increasing binding of BSA with an increase in

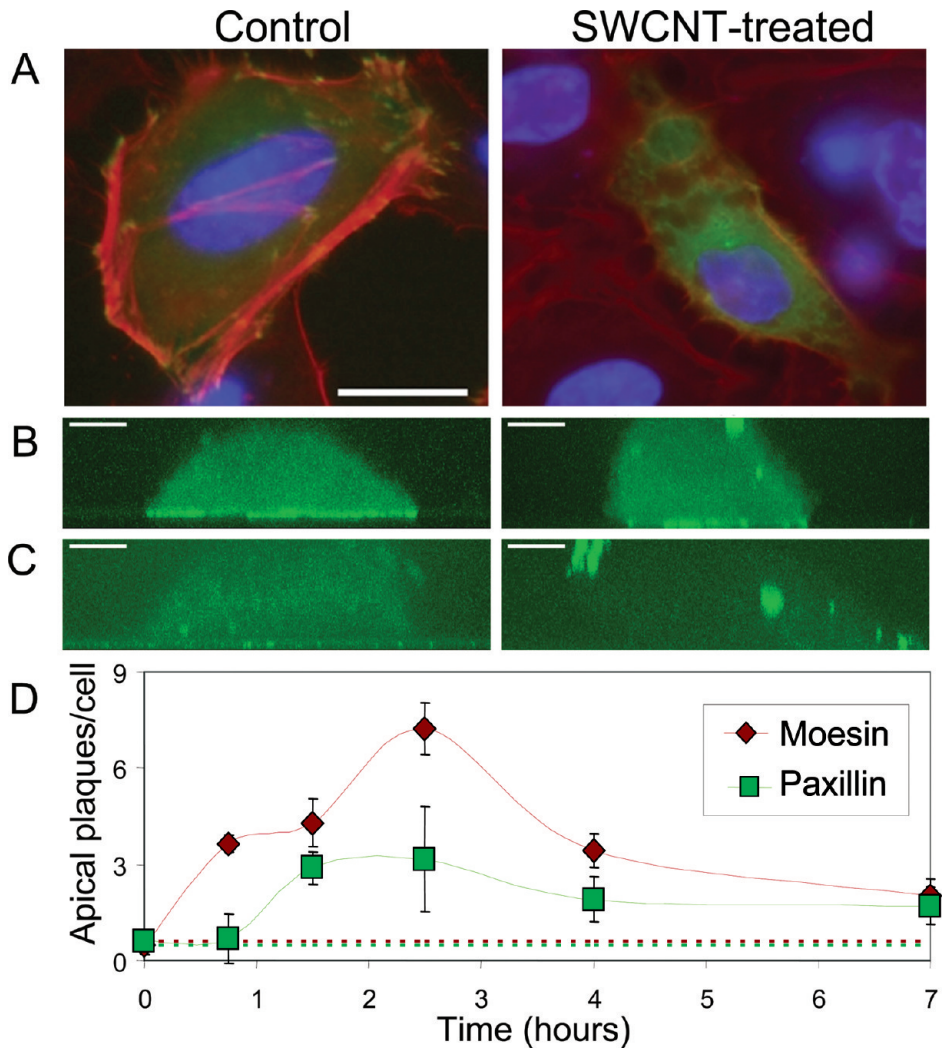

Figure 3. SWCNTs cause early redistribution of actin then paxillin inside cells. (A) At long times, HeLa cells expressing GFP-paxillin normally show punctate focal adhesions (green) at the end of actin stress fibers labeled with rhodamine phalloidin (red). In SWCNT-treated cells (200 μg/mL for 2-days), GFP-paxillin does not localize correctly to punctate focal adhesions (scale 25 μm). (B) At short times of treatment (under 6 h), cells expressing GFP-paxillin imaged in $x-z$ show relocalization of plaques to the apical level of the cell. (C) GFP-moesin, which labels actin but does not alter levels of actin expression,[31] shows actin normally along the basal level of the cells is relocalized to apical plaques (scale 5 μm). (D) Quantification of short-time redistribution of actin (by GFP-moesin, red) and paxillin (by GFP-paxillin, green) shows that actin structures are reorganized within the cell in under an hour, whereas paxillin is unchanged. With increased time paxillin showed reorganization, but the redistribution was less severe than actin (error bars are SEM with $n > 10$ per point).

added SWCNTs (Supporting Information, Figure 4) suggesting a preferred interaction between SWCNTs and F-actin. Labeling of *ex vivo* actin filaments with rhodamine phalloidin and imaging using confocal microscopy showed that these SWCNT-induced actin bundles displayed an anisotropic alignment (Figure 5B). Rhodamine phalloidin-labeled actin networks cross-linked with α-actinin were visualized by confocal microscopy as isotropic networks, in agreement with previous work.[20]

Nanomaterials are Chronically Toxic Materials. Nanomaterials such as SWCNTs have rich technological potential, but their impact on human health is still unknown. By understanding potentially hazardous conditions, proper safety measures can be initiated for production, handling, and disposal. Inert nanomaterials may be small enough to be ignored by the organism's foreign body and immune response or by cellular responses, but we have observed that SWCNTs accumulate in the cells and interfere with cellular processes. The dramatic phenotype observed in SWCNT-treated cells also raises the question on how to define "toxicity". We observed no acute cell death, but a reduction in cell proliferation can be seen as a significant environmental hazard. Here, high concentrations of SWCNTs bundle actin filaments, reorder actin inside the cell, and reduce cell proliferation. The potential long-term, bioaccumulative effects warrant prudent consideration for the use of SWCNTs and nanomaterials in general for widespread technological applications.

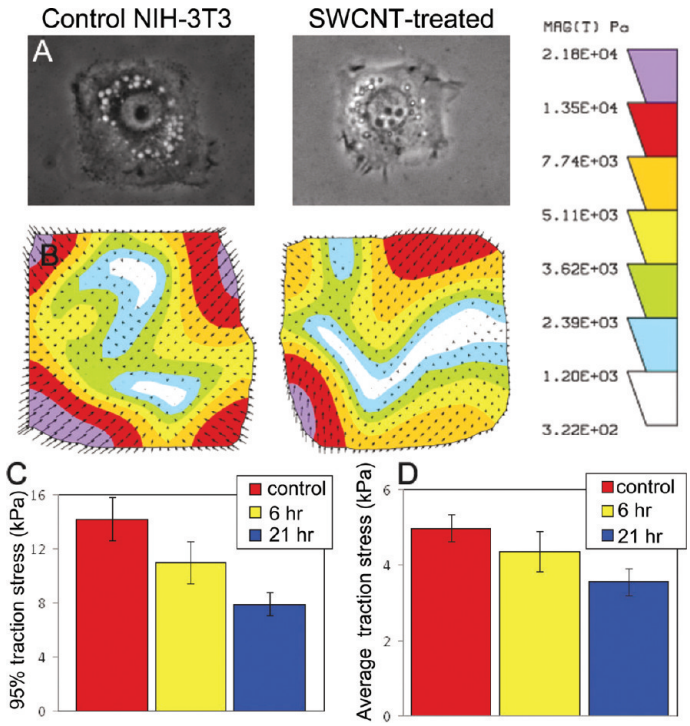

Figure 4. SWCNT-treated fibroblasts generate less stress than control cells. (A) NIH-3T3 cells were cultured on polyacrylamide hydrogels embedded with fluorescent particles coated with a molecular layer of gelatin. These cells, which grew only on the gelatin squares, were then treated with SWCNTs at 200 μg/mL for up to 1 day. When cells were manually removed from the substrate with a microneedle, the translocations of the embedded particles were mapped to cellular stresses.[19] (A) Phase-contrast images of control and SWCNT-treated cells show that the cells are well-adhered, spread on the surface, and take the shape of the pattern. (B) Cell stress vectors, with directions shown with arrows and magnitudes represented with the intensity color maps. (C) Maximum stresses of multiple cells tested were reduced with increased time of SWCNT treatment. A 95% traction stress refers to the highest percentile of stresses, that is, the highest 5% of stresses ($p < 0.001$ at 21 h). (D) The traction stresses averaged over whole cells were also significantly reduced ($p < 0.005$ at 21 h). Error bars are SEM with $n = 16$ for treated cells and $n = 20$ control cells.

Possible Mechanisms of SWCNT—Actin Interactions. Phalloidin can only bind to actin filaments between actin monomers.[21] Since the images from optical microscopy showed that actin was able to form filaments in the presence of SWCNTs, we do not think that SWCNTs induce any structural changes in the actin monomer. Furthermore, fluorescence of pyrene—actin kinetic experiments showed that the rate of actin polymerization was not affected by SWCNTs (Supporting Information, Figure 5), suggesting that SWCNTs interact with actin filaments but not strongly with actin monomers. We suggest that there is likely a weak binding enthalpy between the polymer-coated SWCNTs and the actin filaments. While we have seen no evidence of strong protein binding to SWCNTs (*e.g.*, BSA, G-actin), even a slightly preferential binding energy between actin monomers and SWCNTs would be amplified by the increased contact area along the length of actin filaments and SWCNTs since both molecules are anisotropic and of similar sizes.[22] Any such actin—SWCNT interaction in the cell would be accentuated over other protein or macromolecule interactions due to the high concentration, anisotropy, and remodeling speed of actin. Also, immediately after entering the cell, SWCNTs have the most access to actin of any anisotropic or polymeric macromolecule, which may facilitate this nonspecific interaction.

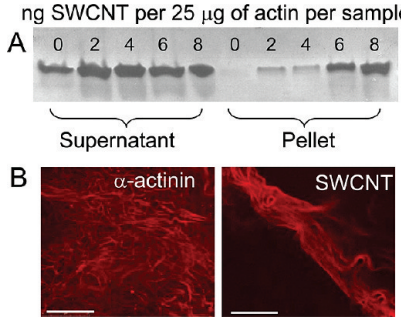

Figure 5. SWCNTs interact with purified actin systems and bundle actin filaments. (A) In a low-speed centrifugation assay, SWCNTs bundle actin filaments increasingly in a dose-dependent way. In the absence of SWCNTs, no actin was pelleted at 12000*g*, whereas at 2, 4, 6, and 8 ng of SWCNT increasing amounts of actin were bundled and were present in the pellet. (B) We also imaged SWCNT-induced actin bundles using confocal microscopy. Cross-linking of actin by α-actinin caused an isotropic network to form. In contrast, SWCNT-induced actin cross-linking led to bundles to occur, most likely due to the anisotropic nature of the SWCNTs. Scale bar in each image is 25 μm.

Other Uses for Actin-Modifying Materials. We also observed that purified and dispersed SWCNTs can induce dramatic anisotropic actin bundle formation both in cells and *ex vivo*. Disrupting or remodeling of F-actin structures can greatly alter cell functions, and targeting F-actin has the potential to provide novel disease therapies. Thus far, naturally occurring substances such as actin stabilizers such as Jasplakinolide,[23] actin depolymerizing agents such as Latrunculin A and cytochalasin D,[24] and actin remodelers such as gelsolin[25] have been utilized to modify actin organization and have been widely used in cell biology, cell mechanics and biophysics research.[24] However, a lack of cell-specific targeting has prevented their application in medical treatments including anticancer therapies since nonspecific actin reorganization within an organism would be disastrous.[26]

SUMMARY

SWCNT-treated cells showed greatly reduced cell proliferation with an increased actin-related division defects, but did not show acute cell death including necrosis and late apoptosis. Images obtained using laser scanning confocal microscopy show that actin, normally present in basal stress fibers in control cells, is located in heterogeneous structures throughout the SWCNT-treated cell. This dramatic reorganization of actin using synthetic molecules within a cell, while not grossly disrupting cell shape or causing apoptosis, represents a novel tool for probing fundamental cellular properties. The potential for biotechnological advances,

such as cancer therapies, by studying targetable moieties that can selectively stop cellular division but not cause death or elicit the immune responses is extremely promising. Unlike many natural small molecules, SWCNTs and the polymer coating can both be modified for targeting.

MATERIALS AND METHODS

SWCNT Purification, Dispersion, and Length Separation. The SWCNT sample was HiPCO (high-pressure carbon monoxide conversion synthesis) and was obtained in unpurified form from Carbon Nanotechnologies, Inc. The unpurified nanotube sample contained SWCNTs as well as carbonaceous impurities (*e.g.*, amorphous carbon, graphitic materials, fullerenes, *etc.*) and remnant metal catalyst particles. The SWCNT sample was purified according to previously described procedures.[9,27] A combination of thermogravimetric analysis and wide-angle X-ray scattering measurements indicated that the purified SWCNT sample contained <5 wt % carbonaceous impurities, ~0.3% metallic impurities, and the rest SWCNTs.[27] The purification process did not change the structure or properties of SWCNTs.[9] To fractionate SWCNTs by length to obtain nanotubes with length of ~150 nm,[17] we dispersed purified SWCNTs in water using sodium deoxycholate (DOC; Aldrich, Inc.) according to previously described procedures.[28] The DOC-stabilized SWCNT dispersions contained a mixture of dispersed and bundles of nanotubes. To separate individual nanotubes from bundles, we centrifuged the DOC-SWCNT dispersions for 2 h at 21000*g* and collected the supernatant.[29] The isolated SWCNTs in the supernatant were then fractionated by length using a density gradient.[30] SWCNTs in the 10th to 12th fractions generally had an average length of ~150 nm. We then pelleted the length-fractionated DOC-stabilized SWCNTs, burned off the DOC by heating the pellet to 300 °C in wet air in the presence of H_2O_2, and then washed in water several times.

The purified and length fractionated SWCNTs were dispersed in water using Pluoronic F127 (BASF), a biocompatible triblock copolymer with the block segments being polyethylene oxide (PEO)−polypropylene oxide (PPO)−PEO. These types of polymers are FDA approved and are routinely used in the pharmaceutical industry, and F127 has been previously shown to optimally disperse SWCNTs.[28] The ratio of SWCNTs to F127 was 1:10 by weight for all the samples. The F127-stabilized nanotube dispersions contained both isolated and bundled nanotubes. To remove the bundles and to collect isolated F127-stabilized SWCNTs, we centrifuged the SWCNT dispersions at 21,000*g* and collected the supernatant. The sharp van Hove peaks (Supporting Information, Figure 6) in the absorption spectra from the supernatant confirmed that SWCNTs were isolated in the supernatant.[29] The concentration of F127 stabilized SWCNTs in the supernatant was determined using near-infrared (NIR) spectroscopy and an extinction coefficient of 2.6 (absorbance mL)/(mg mm) at 930 nm.[30] The supernatant was diluted as needed and used immediately for all experiments. The F127 stabilized SWCNT solutions were stable for several days even after being diluted with large levels of water or physiological levels of salt.

Cell Culture, Transfection, and SWCNT-Treatment. To measure the cellular effects of SWCNTs, HeLa cells were cultured in cell culture media (Dubelco's modified eagle media, 10% fetal bovine serum, 1% penicillin−streptomycin; all from Invitrogen) in 6-well plates, seeded at 2×10^5 (for toxicity studies) and 5×10^4 (for proliferation studies) cells/well. For studies involving expression of GFP-tagged exogenous proteins, HeLa cells were transfected with GFP-paxillin or GFP-moesin[31] 24 h prior to treatment using Polyfect (Qiagen, Inc.) per manufacturer's recommendations. Cells were plated 24 h prior to SWCNT treatment and were washed once with phosphate buffer saline (PBS; Invitrogen).

SWCNTs were sterilized under a UV lamp for 1 h, diluted in PBS and added to cells for 2 h. Media was then added (without washing) to the well, and cells/SWCNTs were incubated together. After 2 days, the media (and residual, suspended SWCNTs) was collected and checked for residual cells and cellular debris by centrifugation, resuspension, and visualization on a microscope.

Cytotoxicity, Proliferation, And Cellular Labeling. PBS with PI, a cell impermeable nucleic acid stain, and Hoechst 33342, a cell permeable nucleic acid stain, were added to each well. PI, a measure of dead cells, fluoresces red and Hoechst 33342, a measure of all cells, fluoresces blue. Images were taken at 20× in the red and blue channels. The data were analyzed using ImageJ to count the number of bright, segmented spots per image. Toxicity and proliferation imaging experiments were repeated in triplicate, typically with more than 1000 cells per experiment, depending on proliferation rate. For high resolution imaging of actin filaments and nuclear structures, cells were fixed with 3.7% formaldehyde in PBS, permeabilized with 0.2% triton X-100 in PBS, blocked with 2% BSA in PBS, and stained with 0.25 μg/mL 4′,6-diamidino-2-phenylindole, dihydrochloride (DAPI) for DNA and 0.165 μM rhodamine phalloidin for F-actin.

Traction Force Microscopy. Micropatterning of polyacrylamide gels was achieved using microcontact printing, described in detail elsewhere.[32] Briefly, a micropattern of gelatin was created on a coverslip by microcontact printing, then transferred to the surface of a sheet of 5% polyacrylamide with 0.1% bis-acrylamide (both from BioRad) containing a 1:1000 dilution of fluorescent latex microbeads (Invitrogen). The stiffness of the final polyacrylamide gel was estimated to be 30 kPa.[33] The gel was incubated in cell culture media at 37 °C for 30 min, and then the cells were seeded. Cells were allowed to adhere and spread overnight, and then treated with SWCNTs.

Traction force microscopy was conducted as described previously.[19] Briefly, a phase contrast image of a single cell adhered and fully spread on a square was acquired followed by a fluorescence picture of the beads directly underneath the cell. The cell was manually removed with a microneedle, and a second fluorescence picture of the beads was taken. Substrate displacement fields and traction maps were computed using the LIBTRC package as described previously (courtesy of Dr. Micah Dembo, Boston University).[19]

***Ex Vivo* Actin Bundling Assay.** G-Actin at 0.25 mg/mL, preincubated with ATP for 30 min, was polymerized with the addition of 1 mM ATP, 50 mM KCl, and 2 mM $MgCl_2$ at room temperature as per manufacturer's instructions (from Cytoskeleton kit BK001) in the presence of SWCNTs. Samples were then centrifuged at 12000*g* or were added to fluorescent dyes for imaging. Centrifugation at 12000*g* does not pellet SWCNTs, SWCNTs incubated with BSA (Supporting Information, Figure 4), or actin alone.[20] After centrifugation, F-actin bundled by SWCNTs was found in the pellet, whereas un-cross-linked F-actin was found in the supernatant. Polyacrylamide gel electrophoresis (12% SDS-PAGE gels from Bio-Rad) of reduced samples was used to visualize actin in the supernatant or pellet.[20] It should be noted that higher concentrations of SWCNTs had a more dramatic bundling effect but had deleterious effects on the polyacrylamide gel. Imaging of bundled samples was performed by polymerizing actin filaments with SWCNT samples on coverslips which had 3 μL of rhodamine phalloidin diluted in 7 μL of methanol dried onto coverslips.

Optical Imaging. Unless otherwise specified, widefield imaging was performed on a DMI6000B inverted fluorescence microscope from Leica with 20× (0.4 NA) dry and 63× (1.4 NA) oil immersion objectives and cooled charged couple device (CCD) camera. Random areas were selected for toxicology and proliferation assays using the automated *xy* stage feature. Confocal imaging was performed using Leica SP5 scanning confocal microscope with 100× oil immersion objective and 2× confocal zoom.

Acknowledgment. We thank D. Kaya for assistance with confocal imaging and L. Davidson for GFP-moesin. We thank M. Dembo of Boston University for providing the LIBTRC package for calculating traction stress. We also acknowledge M. Deserno,

K. Wilson, J. Crocker, and G. Grason for discussions. This work was supported by the NSF (CBET-0708418 & DMR-0619424 (KND and MFI), and DMR-0645596 (MFI)), and the Sloan Foundation (MFI).

Supporting Information Available: Supporting figures: (1) unique cellular phenotypes associated with SWCNT treatment; (2) changes in cell shape and actin reorganization in single cells treated with SWCNTs; (3) reorganized focal adhesions in SWCNT-treated cells; (4) SDS-PAGE gel showing that SWCNTs do not strongly bind nonspecifically to BSA; (5) pyrene actin fluorescence assay showing that SWCNTs do not affect actin polymerization; (6) absorption spectra of isolated SWCNTs stabilized in water using a triblock copolymer Pluronic F127. This material is available free of charge *via* the Internet at http://pubs.acs.org.

REFERENCES AND NOTES

1. Kam, N. W.; Dai, H. Carbon Nanotubes as Intracellular Protein Transporters: Generality and Biological Functionality. *J. Am. Chem. Soc.* **2005**, *127*, 6021–6026.
2. Lu, Q.; Moore, J. M.; Huang, G.; Mount, A. S.; Rao, A. M.; Larcom, L. L.; Ke, P. C. RNA Polymer Translocation with Single-Walled Carbon Nanotubes. *Nano Lett.* **2004**, *4*, 2473–2477.
3. Fakhri, N.; Tsyboulski, D. A.; Cognet, L.; Weisman, R. B.; Pasquali, M. Diameter-Dependent Bending Dynamics of Single-Walled Carbon Nanotubes in Liquids. *Proc. Natl. Acad. Sci. U.S.A.* **2009**, *106*, 14219–14223.
4. Jin, H.; Heller, D. A.; Sharma, R.; Strano, M. S. Size-Dependent Cellular Uptake and Expulsion of Single-Walled Carbon Nanotubes: Single Particle Tracking and a Generic Uptake Model for Nanoparticles. *ACS Nano* **2009**, *3*, 149–158.
5. Jin, H.; Heller, D. A.; Strano, M. S. Single-Particle Tracking of Endocytosis and Exocytosis of Single-Walled Carbon Nanotubes in NIH-3T3 Cells. *Nano Lett.* **2008**, *8*, 1577–1585.
6. Liu, Z.; Davis, C.; Cai, W.; He, L.; Chen, X.; Dai, H. Circulation and Long-Term Fate of Functionalized, Biocompatible Single-Walled Carbon Nanotubes in Mice Probed by Raman Spectroscopy. *Proc. Natl. Acad. Sci. U.S.A.* **2008**, *105*, 1410–1415.
7. Welsher, K.; Liu, Z.; Daranciang, D.; Dai, H. Selective Probing and Imaging of Cells with SingleWalled Carbon Nanotubes as Near-Infrared Fluorescent Molecules. *Nano Lett.* **2008**, *8*, 586–590.
8. Kolosnjaj, J.; Szwarc, H.; Moussa, F. Toxicity Studies of Carbon Nanotubes. *Adv. Exp. Med. Biol.* **2007**, *620*, 181–204.
9. Johnston, D. E.; Islam, M. F.; Yodh, A. G.; Johnson, A. T. Electronic Devices Based on Purified Carbon Nanotubes Grown by High-Pressure Decomposition of Carbon Monoxide. *Nat. Mater.* **2005**, *4*, 589–592.
10. Shvedova, A. A.; Castranova, V.; Kisin, E. R.; Schwegler-Berry, D.; Murray, A. R.; Gandelsman, V. Z.; Maynard, A.; Baron, P. Exposure to Carbon Nanotube Material: Assessment of Nanotube Cytotoxicity Using Human Keratinocyte Cells. *J. Toxicol. Environ. Health A* **2003**, *66*, 1909–1926.
11. Luoto, K.; Holopainen, M.; Perander, M.; Karppinen, K.; Savolainen, K. M. Cellular Effects of Particles-Impact of Dissolution on Toxicity of Man-Made Mineral Fibers. *Cent. Eur. J. Public Health* **1996**, *4*, 29–32.
12. Cui, D.; Tian, F.; Ozkan, C. S.; Wang, M.; Gao, H. Effect of Single Wall Carbon Nanotubes on Human HEK293 Cells. *Toxicol. Lett.* **2005**, *155*, 73–85.
13. Kaiser, J. P.; Wick, P.; Manser, P.; Spohn, P.; Bruinink, A. Single Walled Carbon Nanotubes (SWCNT) Affect Cell Physiology and Cell Architecture. *J. Mater. Sci. Mater. Med.* **2008**, *19*, 1523–1527.
14. Liu, D.; Yi, C.; Zhang, D.; Zhang, J.; Yang, M. Inhibition of Proliferation and Differentiation of Mesenchymal Stem Cells by Carboxylated Carbon Nanotubes. *ACS Nano* **2010**, *4*, 2185–2195.
15. Singh, R.; Pantarotto, D.; McCarthy, D.; Chaloin, O.; Hoebeke, J.; Partidos, C. D.; Briand, J. P.; Prato, M.; Bianco, A.; Kostarelos, K. Binding and Condensation of Plasmid DNA onto Functionalized Carbon Nanotubes: Toward the Construction of Nanotube-Based Gene Delivery Vectors. *J. Am. Chem. Soc.* **2005**, *127*, 4388–4396.
16. Zhang, X.; Meng, L.; Lu, Q.; Fei, Z.; Dyson, P. J. Targeted Delivery and Controlled Release of Doxorubicin to Cancer Cells Using Modified Single Wall Carbon Nanotubes. *Biomaterials* **2009**, *30*, 6041–6047.
17. Becker, M. L.; Fagan, J. A.; Gallant, N. D.; Bauer, B. J.; Bajpai, V.; Hobbie, E. K.; Lacerda, S. H.; Migler, K. B.; Jakupciak, J. P. Length-Dependent Uptake of DNA-Wrapped Single-Walled Carbon Nanotubes. *Adv. Mater.* **2007**, *19*, 939–945.
18. Cao, L. G.; Wang, Y. L. Mechanism of the Formation of Contractile Ring in Dividing Cultured Animal Cells. I. Recruitment of Preexisting Actin Filaments into the Cleavage Furrow. *J. Cell Biol.* **1990**, *110*, 1089–1095.
19. Dembo, M.; Wang, Y. L. Stresses at the Cell-to-Substrate Interface During Locomotion of Fibroblasts. *Biophys. J.* **1999**, *76*, 2307–2316.
20. Shin, J. H.; Gardel, M. L.; Mahadevan, L.; Matsudaira, P.; Weitz, D. A. Relating Microstructure to Rheology of a Bundled and Cross-Linked F-Actin Network *in Vitro*. *Proc. Natl. Acad. Sci. U.S.A.* **2004**, *101*, 9636–9641.
21. Oda, T.; Namba, K.; Maeda, Y. Position and Orientation of Phalloidin in F-Actin Determined by X-ray Fiber Diffraction Analysis. *Biophys. J.* **2005**, *88*, 2727–2736.
22. Leckband, D. E. The Influence of Protein and Interfacial Structure on the Self-Assembly of Oriented Protein Arrays. *Adv. Biophys.* **1997**, *34*, 173–190.
23. Bubb, M. R.; Senderowicz, A. M.; Sausville, E. A.; Duncan, K. L.; Korn, E. D. Jasplakinolide, a Cytotoxic Natural Product, Induces Actin Polymerization and Competitively Inhibits the Binding of Phalloidin to F-Actin. *J. Biol. Chem.* **1994**, *269*, 14869–14871.
24. Rotsch, C.; Radmacher, M. Drug-Induced Changes of Cytoskeletal Structure and Mechanics in Fibroblasts: An Atomic Force Microscopy Study. *Biophys. J.* **2000**, *78*, 520–535.
25. Cunningham, C. C.; Stossel, T. P.; Kwiatkowski, D. J. Enhanced Motility in NIH 3T3 Fibroblasts that Overexpress Gelsolin. *Science* **1991**, *251*, 1233–1236.
26. Senderowicz, A. M.; Kaur, G.; Sainz, E.; Laing, C.; Inman, W. D.; Rodriguez, J.; Crews, P.; Malspeis, L.; Grever, M. R.; Sausville, E. A.; *et al.* Jasplakinolide's Inhibition of the Growth of Prostate Carcinoma Cells *in Vitro* with Disruption of the Actin Cytoskeleton. *J. Natl. Cancer Inst.* **1995**, *87*, 46–51.
27. Islam, M. F.; Milkie, D. E.; Torrens, O. N.; Yodh, A. G.; Kikkawa, J. M. Magnetic Heterogeneity and Alignment of Single Wall Carbon Nanotubes. *Phys. Rev. B* **2005**, *71*, 201401.
28. Islam, M. F.; Rojas, E.; Bergey, D. M.; Johnson, A. T.; Yodh, A. G. High Weight Fraction Surfactant Solubilization of Single-Wall Carbon Nanotubes in Water. *Nano Lett.* **2003**, *3*, 269–273.
29. Arnold, M. S.; Green, A. A.; Hulvat, J. F.; Stupp, S. I.; Hersam, M. C. Sorting Carbon Nanotubes by Electronic Structure Using Density Differentiation. *Nat. Nanotechnol.* **2006**, *1*, 60–65.
30. Fagan, J. A.; Becker, M. L.; Chun, J.; Hobbie, E. K. Length Fractionation of Carbon Nanotubes Using Centrifugation. *Adv. Mater.* **2008**, *20*, 1609–1613.
31. Litman, P.; Amieva, M. R.; Furthmayr, H. Imaging of Dynamic Changes of the Actin Cytoskeleton in Microextensions of Live NIH3T3 Cells with a GFP Fusion of the F-Actin Binding Domain of Moesin. *BMC Cell Biol.* **2000**, *1*, 1.
32. Bernard, A.; Delamarche, E.; Schmid, H.; Michel, B.; Bosshard, H. R.; Biebuyck, H. Printing Patterns of Proteins. *Langmuir* **1998**, *14*, 2225–2229.
33. Munevar, S.; Wang, Y.; Dembo, M. Traction Force Microscopy of Migrating Normal and H-ras Transformed 3T3 Fibroblasts. *Biophys. J.* **2001**, *80*, 1744–1757.